Monthly Notices
of the
ROYAL ASTRONOMICAL SOCIETY

MNRAS **477,** 1308–1317 (2018)
Advance Access publication 2018 March 23

doi:10.1093/mnras/sty777

# On the age of the Nele asteroid family

V. Carruba,[1,2]★ D. Vokrouhlický,[3] D. Nesvorný[2] and S. Aljbaae[1]

[1]*School of Natural Sciences and Engineering, São Paulo State University (UNESP), Guaratinguetá - SP 12516-410, Brazil*
[2]*Department of Space Studies, Southwest Research Institute, Boulder, CO 80302, USA*
[3]*Institute of Astronomy, Charles University, V Holešovičkách 2, CZ-18000 Prague 8, Czech Republic*

Accepted 2018 March 15. Received 2018 March 13; in original form 2018 February 8

**ABSTRACT**

The Nele group, formerly known as the Iannini family, is one of the youngest asteroid families in the main belt. Previously, it has been noted that the pericentre longitudes $\varpi$ and nodal longitudes $\Omega$ of its largest member asteroids are clustered at the present time, therefore suggesting that the collisional break-up of parent body must have happened recently. Here, we verify this conclusion by detailed orbit-propagation of a synthetic Nele family and show that the current level of clustering of secular angles of the largest Nele family members requires an approximate age limit of 4.5 Myr. Additionally, we make use of an updated and largely extended Nele membership to obtain, for the first time, an age estimate of this family using the backward integration method. Convergence of the secular angles in a purely gravitational model and in a model including the non-gravitational forces caused by the Yarkovsky effect are both compatible with an age younger than 7 Myr. More accurate determination of the Nele family age would require additional data about the spin state of its members.

**Key words:** minor planets, asteroids: general – minor planets, asteroids: individual: Nele– celestial mechanics.

## 1 INTRODUCTION

Asteroid families form as a result of collisions among asteroids. The orbits of fragments originating from each break-up event subsequently evolve due to gravitational and non-gravitational effects such as planetary perturbations and the Yarkovsky effect (Bottke et al. 2002; Vokrouhlický et al. 2015). The present orbital distribution of family members is therefore a combination of the initial spread produced by the original ejection velocity field and later dynamical evolution. Separating the two effects is often difficult, because the velocity field is a priori unknown and because the strength of the Yarkovsky effect depends on various parameters, such as the asteroid density and surface thermal conductivity, that are poorly constrained.

Young asteroid families (i.e. families that formed less than ∼20 Myr ago) are useful in this context, because of our ability to precisely model the dynamics of asteroids on short time-scales. For example, in the case of a young asteroid family it is often possible to demonstrate the past convergence of the pericentre longitudes $\varpi$ and nodal longitudes $\Omega$. Such a convergence is expected because the ejection velocities are typically only a small perturbation of the orbital speed. All fragments should therefore have about the same values of $\varpi$'s and $\Omega$'s immediately after the parent body break-up, which becomes apparent when the orbits of young family members are integrated backward in time from the present epoch (e.g. Nesvorný et al. 2002; Nesvorný et al. 2003).

Modelling young families provides valuable information about their age and membership. It may also help to constrain key parameters of the Yarkovsky effect, because the Yarkovsky effect needs to be taken into account to precisely reconstruct the past convergence of angles (e.g. Nesvorný & Bottke 2004). In some cases, such as for the Karin cluster, it was even shown that strict convergence criteria allow for a detection of the radiation torque known as the YORP effect (Carruba, Nesvorný & Vokrouhlický 2016).

In this work, we focus our attention on the case of the Nele cluster (family identification number, or FIN, 520 in Nesvorný, Brož & Carruba 2015). This family, previously also known as the Iannini family, was suggested to be younger than 5 Myr in Nesvorný et al. (2003), because the $\varpi$'s and $\Omega$'s of its members were found to be clustered even at the present epoch. Using a larger data set of numbered and multi-opposition asteroids for which the proper orbital elements were determined, Milani et al. (2014) recently found that (1547) Nele is likely the largest member in the former Iannini cluster and thus opted to rename the cluster after this body. We adopt this point of view, but readers should be aware of the previous name used for this group, if necessary. Here, we take advantage of a still larger data set of asteroids for which proper orbital elements were determined and made available at the AstDyS website in 2017 June to extend and improve the analysis of both Nesvorný et al. (2003) and Milani et al. (2014). More importantly, using methods also developed in Carruba, Nesvorný & Vokrouhlický (2016) and

★ E-mail: valerio.carruba@unesp.br

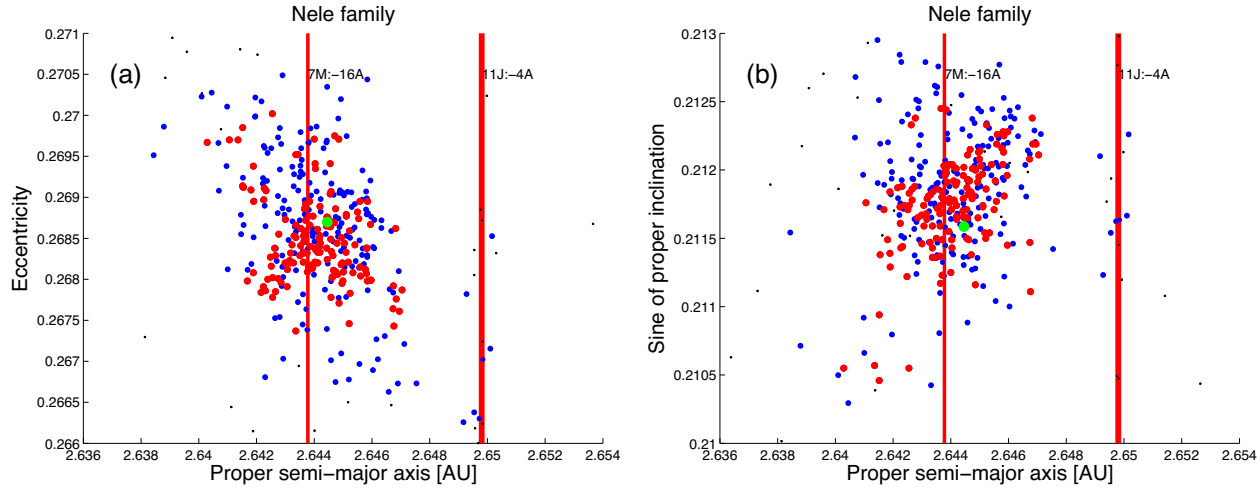


**Figure 1.** Proper elements, ($a$, $e$) in panel (a) and ($a$, $\sin i$) in panel (b), of Nele family members (blue dots) and background asteroids (black dots). For comparison, the red dots display the orbital location of the Iannini asteroid family, as available from Nesvorný et al. (2015). The large full green dot shows the orbital location of (1547) Nele itself. The vertical lines display the location of the principal mean motion resonances in the region.

Carruba, Vokrouhlický & Nesvorný (2017) for the Karin and Veritas families, we demonstrate the past convergence of secular angles of asteroids in the Nele family, and obtain an age estimate of this family using the direct backward orbit integration of its members.

## 2 FAMILY IDENTIFICATION AND DYNAMICAL PROPERTIES

Two sets of membership lists are currently available for the Nele family. Nesvorný et al. (2015) used the hierarchical clustering method (HCM; Bendjoya & Zappalà 2002) and a cutoff of 25 m s$^{-1}$ to obtain a family of 150 members, which is $\simeq$8 times more than the 18 members available at the time of Nesvorný et al. (2003). This family was still called Iannini in Nesvorný et al. (2015). Preference to this name was based on Nesvorný et al. (2003), who observed that (1547) Nele is offset in proper eccentricity and inclination with respect to location of other large asteroids in this cluster. However, when smaller members were later associated with this cluster in larger data bases, this was no longer the case. For that reason, Milani et al. (2014) proposed to call this cluster the Nele family. Indeed, more recent and quite larger data sets of proper orbital elements that become available at the AstDyS website in 2017 June (http://Hamilton.dm.unipi.it/astdys; Knežević and Milani 2003) confirm this trend. Automated methods of family identification at the AstDyS site have resulted in the detection of 344 members of the Nele family. Observing this evolution, we also adopt the Nele attribution for this family name and basically use the membership available at the AstDyS website, performing the following brief analysis.

The family is very compact and isolated. Using the criteria of Carruba & Nesvorný (2016), we identified objects in the local background of this group. Specifically, we used the synthetic proper elements from the AstDyS site, and selected orbits with values between 0.2663 and 0.2710 in proper $e$ and between 0.2103 and 0.2130 in proper $\sin i$ (four standard deviations of the Nele family distribution around the family barycenter). Values of proper $a$ were chosen from 2.638 to 2.651 au (the family range $\pm$0.02 au). Only 81 additional background objects were found using this method (atop to the 344 identified Nele members). These additional asteroids were found to be randomly scattered in the selected box of proper orbital elements showing no tendency of clustering. This indicates that these background asteroids are, most likely, not family members and we will not include them in the following analysis. Using HCM for objects in this local background, we found that 92.7 per cent of the 425 asteroids in the region join the Nele family for cutoff values of 50 m s$^{-1}$. All asteroids become members of the family for cutoff values larger than 75 m s$^{-1}$.

The Milani et al. (2014) and Nesvorný et al. (2015) families are shown in Fig. 1. We identified all secular resonances up to order six in the Nele family region, but no member of the family was found in a secular resonance with planets or massive asteroids. Secular dynamics therefore seems unimportant. Gallardo (2014) identified the 11J-4A resonance with Jupiter at $a \simeq 2.6498$ au and the 7M-16A resonance with Mars at $a \simeq 2.6438$ au as the two main mean motion resonances in the region. The 11J-4A affects seven family members at large-end of the semimajor axis values, but most Nele objects are not significantly affected by either of the resonances.

To better understand the role of chaotic dynamics, we identified asteroids in different ranges of the Lyapunov Characteristics exponents (LCE). The LCE estimates were obtained from AstDyS. Fig. 2 shows objects with LCEs in three different intervals (the figure caption specifies the equivalent limits in terms of the Lyapunov times $T_{\rm L}$, defined as the inverse of LCEs). Apart from the chaotic region associated with the 11J-4A resonance already discussed, three mildly chaotic areas were also found: one at $\simeq$2.6426 au, possibly associated with the 4S-5M+12A three-body resonance, one at $\simeq$2.6444 au, possibly related to the 1S-4M+9A and four-body resonances such as 15J-1S-1M+3A, and one at $\simeq$2.6464 au, which is probably related to the 13J-1M-7A three-body resonance and the 7V-1A two-body resonance with Venus (e.g. Nesvorný et al. 1998; Gallardo 2014). No chaotic region was found at the semimajor axis of the 7M-16A resonance. Both (1547) Nele and (4652) Iannini, the family largest bodies, have mildly chaotic orbits (i.e. $6.7 \times 10^4 < T_{\rm L} < 5 \times 10^5$ yr).

## 3 PHYSICAL PROPERTIES

Nesvorný et al. (2015) listed Iannini as an S-type family, with a mean geometric albedo $p_V$ of 0.32. This analysis is confirmed for the new larger Nele family found by Milani et al. (2014) and recent

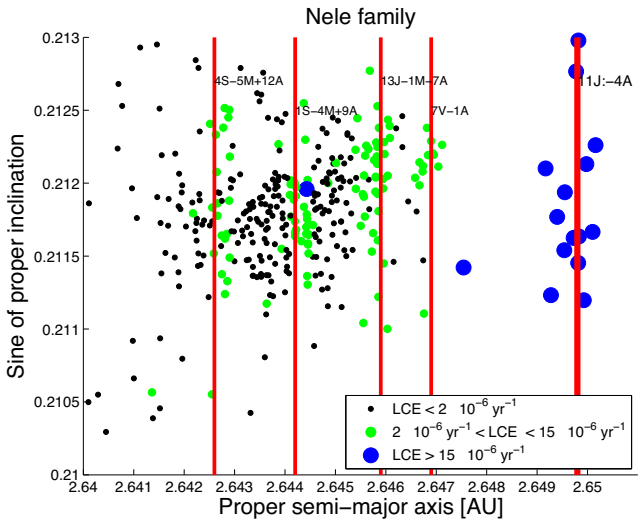


**Figure 2.** A ($a$, $\sin i$) projection of asteroids in the local background of the Nele family. Objects with Lyapunov times $T_L$ longer than $5 \times 10^5$ yr are shown as black dots (these are the most stable orbits). Objects with $6.7 \times 10^4 < T_L < 5 \times 10^5$ yr are displayed as green full circles, while the objects with $T_L < 6.7 \times 10^4$ yr are shown as blue full circles (for most part affected by the 11J-4A mean motion resonance).

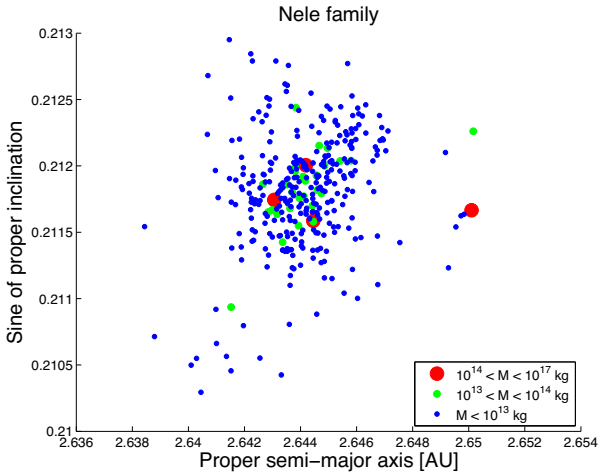


**Figure 3.** An ($a$, $\sin i$) projection of asteroids near the orbital location of the Nele family. The colour and size of the symbols reflect the estimated asteroid mass. Asteroid (43766) 1988 CR4, represented by the large red symbol at $a \simeq 2.65$ au away from the centre of the Nele family and in the 11J-4A resonance, is suggested to be an interloper from the background population of objects.

updates at the AstDyS, which identify this group as an S-type family of a mean albedo 0.355. There is very limited information available about other physical properties of the members of the Nele family. Only seven objects have photometric data in the Sloan Digital Sky Survey-Moving Object Catalog data (SDSS-MOC4; Ivezić et al. 2001) from which the taxonomic information can be obtained using the method of DeMeo & Carry (2013), and only 14 objects have geometric albedo and absolute magnitude information available in the *WISE* and *NEOWISE*, *AKARI*, or *IRAS* data bases (Ishihara et al. 2010; Ryan & Woodward 2010; Masiero et al. 2012; Mainzer et al. 2016).

Of the seven objects with taxonomic information based on broad-band SDSS data, four belong to the S-complex (4652 Iannini, K-type, 78908, Q-type, 146444, S-type, and 161328, S-type), and three to the C-complex (1547 Nele, TD-type, and 151032 and 164726, both C-types). These data do not allow us to reach any conclusion on the taxonomy of the Nele family. Geometric albedo data is more helpful. Of the 14 objects with *WISE* albedo, only two, (185380) and (43766) have an albedo lower than 0.2. The median value of the geometric albedo is of 0.315, and the mean value is equal to 0.293, essentially confirming the analysis of Nesvorný et al. (2015) and Milani et al. (2014). Based on this data, the Nele family is most likely an S-complex family, and the asteroids 151032, 164726, and 185380 are either potential interlopers or objects for which the Sloan-derived taxonomy is misleading. Interestingly, (1547) Nele was classified as a TD object in a Tholen taxonomy based on two colour indexes, but has an albedo of 0.20, barely compatible with that of other family members.

To better understand the distribution of largest members of the family, we estimated the masses assuming objects to be spherical with a bulk density equal to 2500 kg m$^{-3}$ (typical value of S-type objects; this is close to the guessed value of 2275 kg m$^{-3}$ reported at the AstDyS site). For objects with available *WISE* albedo data, we used the *WISE* $p_V$ value to estimate their radius from the absolute magnitude (equation 1 as in Carruba et al. 2003). For all other objects, we used $p_V = 0.315$, which is the median value of this family. Fig. 3 shows the results. Only three objects have estimated masses larger than $10^{14}$ kg and diameters $D > 5$ km and these are (1547) Nele ($D \simeq 17.3$ km), (4652) Iannini ($D \simeq 5.3$ km), and (43766) 1988 CR4 ($D \simeq 7.2$ km). However, the fact that (43766) 1988 CR4 is an albedo outlier of this family and its location in the 11J-4A mean-motion resonance away from other large asteroids in the family both suggest this body is an interloper in the cluster. (81550) 2000 HU23 is the only other object with an estimated mass larger than $10^{14}$ kg, and has a diameter of $\simeq$4.9 km.

## 4 AGE ESTIMATES OF THE NELE FAMILY

Recently, Spoto et al. (2015) estimated the age of the Nele family using the method of V-shape fitting in the domain of semimajor axis and inverse diameters. In this method, the distribution of asteroids is binned for different values of asteroid inverse diameters, and the asteroids with minimum and maximum semimajor axis values are selected. The bin sizes are chosen so that the differences in the number of members in two consecutive bins never exceeds one standard deviation. Errors are assigned on the asteroids inverse diameters, and outliers are rejected using an automatic outliers rejection scheme. The slopes of the two sides of the family V-shape are then computed, with their errors. Ages and their uncertainty are then estimated using a Yarkovsky calibration for the values of the semimajor axis drift rate d$a$/d$t$, based on the radar results for asteroid (101955) Bennu (Chesley et al. 2014, and subsequently rescaled to the family heliocentric location and assumed bulk densities of the members).

Spoto et al. (2015) obtained values of the $1/S$ slope equal to $-0.005 \pm 0.0008$ for the IN inverse slope and of $0.005 \pm 0.002$ for the OUT inverse slope. Once the Yarkovsky calibrations and their errors were accounted for, this corresponds to ages of $14 \pm 5$ and $15 \pm 7$ Myr, respectively. However, observing the suggested age limit of $\simeq$5 Myr from clustering of secular angles in Nesvorný et al. (2003), Spoto et al. (2015) pointed out that the effects of the initial velocity field could be rather important for this very young family (implying that possibly the initial spread of Nele asteroids

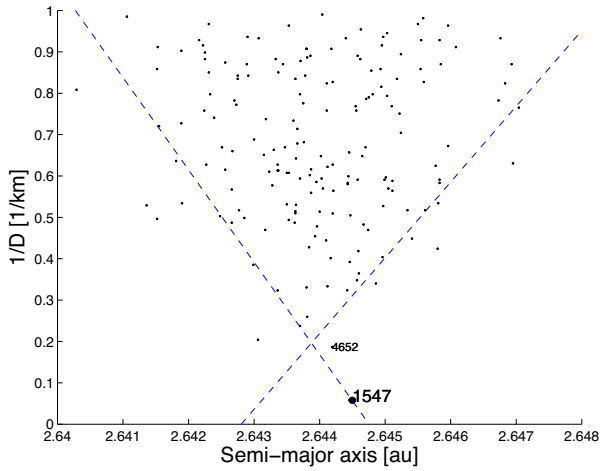


**Figure 4.** The V-shape in the ($a$, $1/D$) domain for the Nele family. The black full dot displays the location of (1547) Nele, largest member in the family.

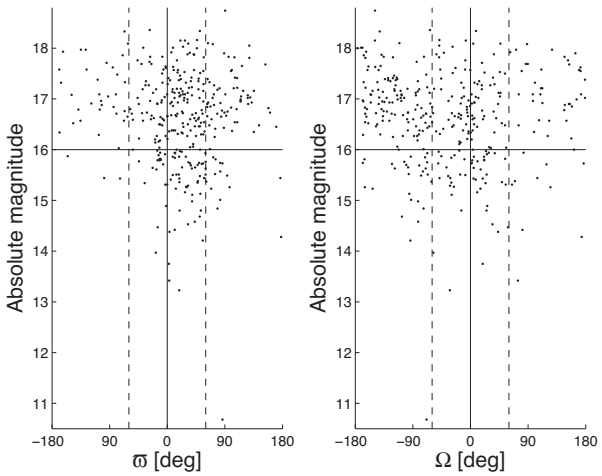


**Figure 5.** The current ($\varpi$, $H$) and ($\Omega$, $H$) distributions of members of the Nele family, where $\varpi$ and $\Omega$ are osculating values at the MJD epoch 57200 and $H$ are absolute magnitudes from AstDyS site. The vertical black lines display $\Omega$ and $\varpi$ equal to 0°, while the vertical dashed line shows the ±60° levels. The horizontal line displays the $H = 16$ level.

dominates their distribution in the V-shape domain rather than the Yarkovsky effect, typical for older families).

In order to check these conclusions with more members available, we repeated Spoto et al. (2015) analysis for the Nele family with a similar method.[1] Our results are in good agreement, within the uncertainties, with the solution published by Spoto et al. (2015). Fig. 4 displays the V-shape for the solution using the family centre,[2] and the range of $1/D$ values used for the size binning of the family. We found inverse values of the slopes of $-0.0049 \pm 0.0013$ for the IN slope and of $0.0055 \pm 0.0023$ for the OUT slope.

Taking now an opposite extreme assumption about the spread of Nele family within the bounds of V-lines, we can use the data to obtain an estimate of the initial ejection velocity field. Assuming the initial ejection velocity field was isotropic (at least for small members), the available slopes of the delimiting lines in the ($a$, $1/D$) domain can inform us about the transverse component of the ejection velocity field $V_{\rm T}$. In particular, if $V_{\rm T} \propto 1/D^{\alpha_{\rm EJ}}$ with some exponent $\alpha_{\rm EJ}$, the relationship between the displacement of a particular family member in proper $a$ from the centre $a_{\rm c}$, $|a - a_{\rm c}|$, reads (e.g. Vokrouhlický et al. 2006a,b)

$$|a - a_{\rm c}| = \frac{2}{n} V_{\rm EJ} \left( \frac{D_0}{D} \right)^{\alpha_{\rm EJ}} \cos\theta, \qquad (1)$$

where $n$ is the asteroid mean-motion, $V_{\rm EJ}$ is a parameter that describes the width of the fragment ejection velocity distribution (Vokrouhlický et al. 2006a,b), $D_0$ a reference size value from magnitude–size relationship equal to 1329 km, and $\theta$ is the angle of the fragment ejection velocity relative to the transverse direction of the parent body's orbit. The limits of the V-shape region then correspond to $\cos\theta = \pm 1$. Data for the Karin and Koronis (Nesvorný et al. 2002; Carruba & Nesvorný 2016) families suggest that $\alpha_{EV} \simeq 1$ (see also Bolin et al. 2018). Therefore, if we assume that the V-shape for the Nele family in the ($a$, $1/D$) domain observed in Section 4 is mostly caused by the initial ejection velocity field, the value of the ejection parameter $V_{\rm EJ}$ would be related to the absolute values of the IN and OUT slopes $1/S$ by the relationship

$$V_{\rm EJ} = \frac{n}{2|S|}. \qquad (2)$$

Using the values of $a_{\rm c}$, $S_{\rm IN}$, and $S_{\rm OUT}$ from this section, then $V_{\rm EJ}$ would be 17.2 and 18.4 m s$^{-1}$, respectively. Therefore, this approximate analysis would yield a value of $V_{\rm EJ} = 17.8 \pm 0.6$ m s$^{-1}$, which is similar to the estimated escape velocity from (1547) Nele itself, that is of the order of 10 m s$^{-1}$ (e.g. Brož et al. 2013). Therefore, it is conceivable that at least 2/3 of the asteroid distribution within the V-shape limits is due to the initial velocity field and only 1/3 is the additional component due to the Yarkovsky spreading. With that, both Spoto et al. (2015) and our age estimates mentioned above would shrink to ≃5 Myr.

Now, we come back to the idea of Nesvorný et al. (2003) who suggested an age limit of this cluster from today's distribution of the secular angles of the largest members. Our plan is to carry out a more detailed look into the problem and also check how the secular angles in the Nele family are distributed as a function of their size (now available with much larger data set of its members).

Fig. 5 displays the current ($\Omega$, $H$) and ($\varpi$, $H$) distributions for longitude of node $\Omega$ and longitude of pericentre $\varpi$. The $\varpi$ distribution, and, to a lesser extent, also the $\Omega$ distribution, show tendency to cluster near 0° for members with $H \leq 16$. Smaller members have the secular angles dispersed uniformly in between 0° and 360°. This is expected, because their larger semimajor axis drift $\mathrm{d}a/\mathrm{d}t$ due to the Yarkovsky effect implies an additional contribution in how the secular angles disperse, and, also, smaller fragments tend to be ejected with higher ejection speed, further away from the family centre than larger family members, and would therefore experience larger differences in the precession rates of the secular angles with respect to the parent body than, in general, larger objects. The sample of large members in the family may, therefore, be considered to test the age limit envisaged by Nesvorný et al. (2003).

In order to determine the expected pace at which the secular angles of the orbits in the Nele family diverge, we conducted the following simple numerical experiment. At the current epoch, MJD 57200, we constructed a synthetic cluster of 107 objects around the

[1] Instead of the algorithm used for automatic rejection method used by these authors, we used built-in numerical tools available in MATLAB.

[2] Another solution using (1547) Nele instead is available on the AstDyS as blue curves, but values of the slopes were not available for this solution.

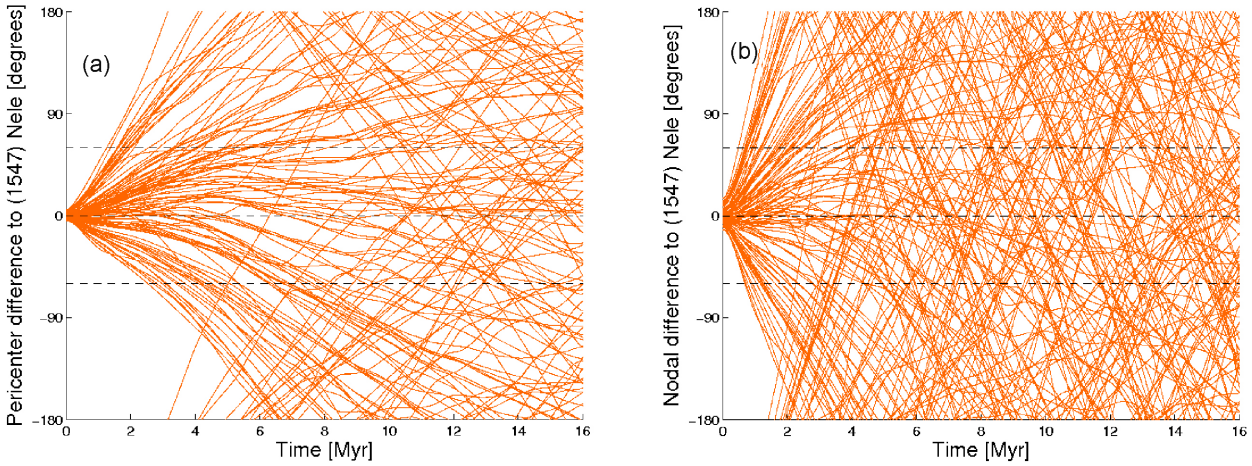


**Figure 6.** The future evolution of the digitally filtered pericentre (panel a) and nodal (panel b) longitudes of 107 Nele members of a synthetic family reproducing conditions after break-up, when purely gravitational forces are considered. The dashed lines show 0° and ±60° for reference.

orbit of (1547) Nele (this corresponds to the $H < 16$ sample, Fig. 5). We used a very conservative velocity ejection speed of 3 m s$^{-1}$ for each of the fragments and assumed they were launched isotropically in space. This renders an initial spread in both longitude of node $\Omega$ and pericentre $\varpi$ of only a fraction of a degree. We intentionally keep the initial velocity small in order not to push the age constraint for the cluster too low.

We numerically integrated the orbits of these objects and computed the filtered values of their difference in $\varpi$ and $\Omega$ with respect to (1547) Nele, with the same procedure discussed in Section 5. The simulation included only gravitational perturbations from the planets, driving circulation of the secular angles, but we neglected the effects of thermal accelerations at this stage. Fig. 6 shows the time behaviour of these differences in $\varpi$ (panel a) and $\Omega$ (panel b) as a function of time. As expected, the distribution of $\Delta\varpi$ and $\Delta\Omega$ starts initially very compact about zero and quickly spreads to become uniform in the whole range of 0° and 360° in a few million years. While the mean rate of the dispersion change in $\varpi$ and $\Omega$ may be estimated analytically, the numerical approach we adopt here is more accurate (note, for instance, that many of the trajectories in Fig. 6 are not straight lines but instead show complex dependence on time, indicating thus chaotic evolution of the orbits).

In order to quantify the secular angles dispersion, we computed the standard deviation of absolute values $|\Delta\varpi|$ and $|\Delta\Omega|$ distributions as a function of time for the simulated family. Fig. 7 displays our results. The horizontal black line indicates the current values of these standard deviations as observed in the sample $H \leq 16$ members of the Nele family (see Fig. 5), while the dashed black lines show the confidence level for the standard deviations of a population of ≃100 asteroids (0.88 SD < SD < 1.16 SD, with SD being the nominal value of the standard deviation; e.g. Sheskin 2003). Values of the standard deviations for a uniform distribution of absolute values are about 51°.5 (e.g. Vokrouhlický et al. 2006b).[3] The results in $\Delta\Omega$ are not conclusive to within the errors. This is because the divergence in $\Omega$ turns out to be quite fast in the zone of Nele family. Mean values of the frequency gradients $\frac{ds}{da}$ for Nele family members are equal to $-101.3 \pm 0.3$ arcsec yr$^{-1}$, which is

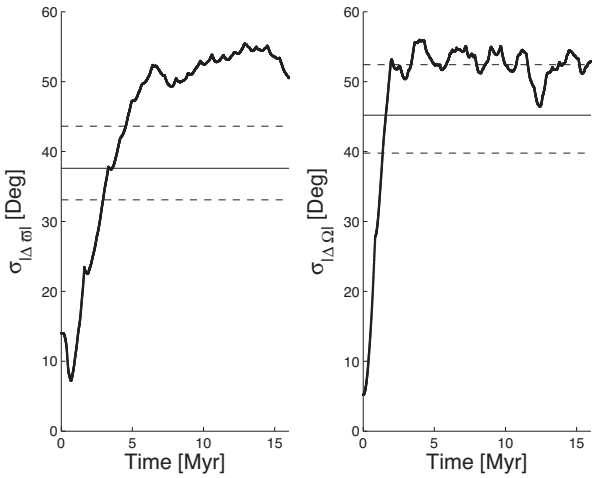


**Figure 7.** Time behaviour of the standard deviation of the absolute values of differences $\Delta\varpi$ and $\Delta\Omega$ in secular angles with respect to (1547) Nele. Data from numerical propagation of 107 members of our synthetic realization of the Nele family started as a compact cluster with 3 m s$^{-1}$ ejection field of fragments. The horizontal black line displays the current value of the standard deviation for the real Nele $H < 16$ members, while the horizontal dashed lines show the confidence level for these values (obtained using methods discussed in Sheskin 2003 for a sample of ≃100 bodies).

higher than what found for the more well-behaved Karin family, for which $\frac{ds}{da} = -70.0 \pm 0.2$ arcsec yr$^{-1}$ (Nesvorný & Bottke 2004). Indeed, the data in Fig. 5 confirm that nodes of even the large bodies in the Nele family are quite spread. Luckily, data in $\varpi$ are more conclusive. The currently observed dispersion $\Delta\varpi \simeq 37°.6$ is attained in our simulation in $3.6^{+0.9}_{-0.7}$ Myr (see panel a in Fig. 6), and, indeed, values of $\frac{dg}{da}$ are relatively small for asteroids in the Nele family ($83.5 \pm 0.4$ compared to $94.3 \pm 0.6$ arcsec yr$^{-1}$ for Karin asteroids). Overall, results of this experiment indicate that the Nele family should indeed be younger of 4.5 Myr, strengthening slightly the suggested limit in Nesvorný et al. (2003).

## 5 PAST CONVERGENCE OF THE SECULAR ANGLES

In this section, we attempt to improve the preliminary age estimates from above by using a direct numerical integration of orbits for Nele

[3] Note that we evaluate angular separation of two angles in our case that is by definition limited to 0°–180°. If we were to consider uniform distribution of only one angle in between 0° and 360°, the limiting standard deviation would be ≃103° as mentioned in Vokrouhlický et al. (2006b).

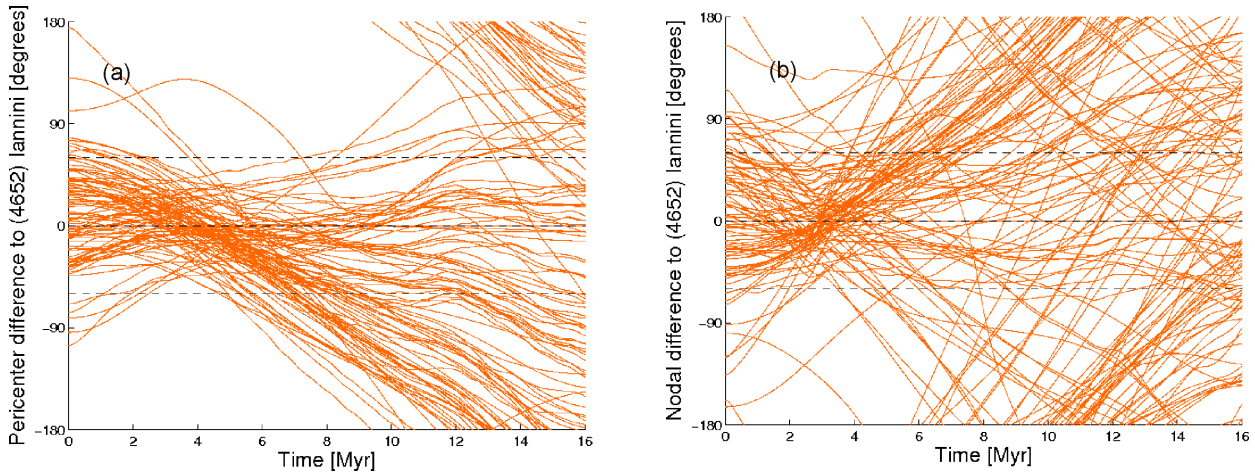


**Figure 8.** The past evolution of the digitally filtered differences in pericentre (panel a) and nodal (panel b) longitudes for the 100 largest Nele members with respect to the orbit of (4652) Iannini (the convergence pattern remains preserved if more asteroid orbits were shown but the figures would get saturated). Only the gravitational perturbations of planets were taken into account in the simulation. The horizontal lines display the 0° and the ±60° levels for reference.

members backward in time and seeking their convergence. Following the approach described in Nesvorný et al. (2003), Nesvorný & Bottke (2004) and Carruba et al. (2016) for the Veritas and Karin families, we first verified the ability to track the convergence of secular angles $\varpi$ and $\Omega$ in the past for 342 Nele members (we excluded two albedo interlopers) by performing a numerical simulation where we only included gravitational perturbations from all planets, Mercury through Neptune, and neglected thermal accelerations known as the Yarkovsky effect. These are expected to become more important for small members in the family. We used the state-of-the-art symplectic integrator known as `SWIFT_MVSF` (e.g. Levison & Duncan 1994) with a 10 d timestep (verifying using a smaller sample of orbits that identical results are obtained for shorter timesteps too). The code was modified by Brož (1999) to include an online filtering of the osculating orbital elements. This function allowed us to obtain both osculating and mean orbital elements at the output from the code.

Following the approach described in Carruba et al. (2016), we considered the case of two reference orbits with respect to which difference $\Delta\varpi$ and $\Delta\Omega$ were computed: (i) (1547) Nele and (ii) (4652) Iannini, the two largest bodies in the family. In an ideal world, which of the reference body is selected should not matter, the choice of the largest fragment is typically justified by expecting the least influence by the non-gravitational effects. In our case, this would be (1547) Nele. However, we have noted above that the pericentre longitude of this body is slightly offset from the values of other large members in the family (see Fig. 5). The reason is not known, but it may be caused by either stochastic effects of close encounters to the most massive bodies in the main belt and/or an asymmetric ejection velocity field with which the largest fragments were launched. Such a slight discrepancy is not observed for (4652) Iannini, the second largest asteroid in the family. This justifies our second choice for the reference orbit. While both result in the same conclusion, we show in Fig. 8 the case of (4652) Iannini as a reference orbit. This is because the data are visually more straightforward to interpret.

To obtain the age estimate for the Nele family, we first computed a $\chi^2$-like variable of the form:

$$\chi_0^2 = \sum_{i=2}^{N_{\rm ast}} ({\Delta\varpi_i}^2 + {\Delta\Omega_i}^2), \tag{3}$$

where $N_{\rm ast}$ is the number of family members, 342, in our case. At this moment, $\chi_0^2$ is plainly a sum of secular angle differences to the reference asteroid and thus has dimension rad$^2$. In our method, the best estimate of the family age corresponds to a minimum in these angular separations $\Delta\varpi_i$ and $\Delta\Omega_i$, or a minimum of the target function given in equation (3). In this case, we use (1547) Nele as a reference body, thus $\Delta\varpi_i = \varpi_i - \varpi_{\rm Nele}$ and $\Delta\Omega_i = \Omega_i - \Omega_{\rm Nele}$. We output our data every $10^3$ yr, but to prevent perturbing effects of a high-frequency noise in $\chi_0^2$ values, both differences were filtered with a low-pass digital Fourier filter. This procedure helped to remove all frequency terms with periods shorter than $10^5$ yr (e.g. Carruba 2010). We tried other reasonable period thresholds in our filtering procedure, but all resulted in very similar conclusions. We also verified that the same results were obtained when the orbit of (4652) Iannini was taken as a reference instead of (1547) Nele.

Once a minimum value of the $\chi_0^2$-like variable is obtained, we estimated the statistical mismatch $\sigma$ of the best-fitting convergence solution taking $\Delta\varpi_i \simeq \Delta\Omega_i \simeq \sigma$. With the definition (3), we have

$$\sigma^2 = \frac{({\chi_0}^2)_{\rm min}}{N_{\rm df}}, \tag{4}$$

where $N_{\rm df} = 2N_{\rm ast} - 3$ is the number of degrees of freedom. Note there were $2(N_{\rm ast} - 1)$ number of pairs contributing by angular differences $\Delta\varpi_i$ and $\Delta\Omega_i$ with respect to the reference orbit, and an additional factor 1 is due to fitting the age of the family. In quantitative terms, we have $({\chi_0}^2)_{\rm min} = 270.3$ rad$^2$ reached at the 3.6 Myr epoch, and thence we obtain $\sigma^2 = 0.397$ rad$^2$. This corresponds to $\sigma \simeq 36\overset{\circ}{.}0$, certainly quite more than the level at which fragments in the Nele family were initially dispersed in either of the secular angles (i.e. a fraction of a degree[4]). At a plain face, we would need to reject the solution. However, we know that the model used is only approximate since it does not take into account fine details such as the thermal accelerations or effects of additional massive bodies in

[4] The value of $\sigma$ may reduce if we eliminate from our sample the asteroids with the largest values of LCE, as also performed by other authors for the Veritas and Theobalda asteroid families (Nesvorný et al. 2003; Novaković 2010). Since, however, in our sample there are just 14 asteroids with *LCE* larger than that of (1547) Nele itself, and since the effect of removing them is to reduce $\sigma$ by just a degree, to $\simeq 34\overset{\circ}{.}9$, we preferred in this work to work with the completed Nele family sample.

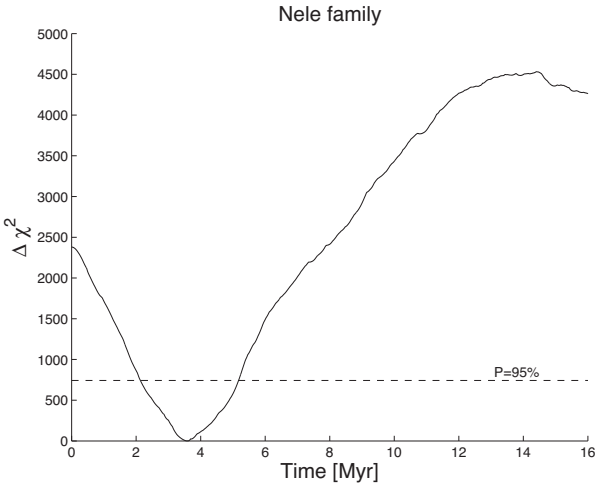


**Figure 9.** The time behaviour of the $\Delta\chi^2 = \chi^2 - \chi^2_{\rm min}$ variable defined in equation (5) for differences in the secular angles with respect to (1547) Nele, filtered with a cutoff of $10^5$ yr. The dashed line shows the 95 per cent probability confidence level defined by $\Delta\chi^2 \simeq 742.8$. The age of the Nele family thus appears to be $3.6 \pm 1.6$ Myr.

the main asteroid belt. As a result, we shall assume that the reached convergence level of $\simeq 36^\circ$ approximately corresponds to the possible limit of our crude model. With this simple approach, we shall adopt that the obtained best-value dispersion $\sigma$ corresponds to the uncertainty of the data points.

This procedure allows us to construct a proper, now non-dimensional $\chi^2$ variable using the relationship

$$\chi^2 = \sum_{i=2}^{N_{\rm ast}} \left[ \left( \frac{\Delta\varpi_i}{\sigma} \right)^2 + \left( \frac{\Delta\Omega_i}{\sigma} \right)^2 \right]. \quad (5)$$

With this target function defined, we formally use the least-squares statistics to determine the single fitted parameter and its formal uncertainty, namely the age of the family. To that end, we construct $\Delta\chi^2 = \chi^2 - \chi^2_{\rm min}$, where $\chi^2_{\rm min} \simeq 1$. Obviously, the formal best-fitting solution of Nele age still corresponds to the epoch where $\chi^2 = \chi^2_{\rm min} \simeq 1$. Confidence level of this solution is set by some choice of $\Delta\chi^2$ value. For instance, the often used 95 per cent confidence level is obtained for $\Delta\chi^2 \simeq 742.8$. This is because our solution has $N_{\rm df} = 2\,N_{\rm ast} - 3 = 679$ degrees of freedom, and the 95 per cent confidence level is obtained from the cumulative distribution function of a $\chi^2$ variable, expressed as

$$F(x, N_{\rm df}) = \frac{\gamma\left(\frac{N_{\rm df}}{2}, \frac{x}{2}\right)}{\Gamma\left(\frac{N_{\rm df}}{2}\right)}, \quad (6)$$

where $x = 0.95$ stands for the chosen confidence level, $\gamma(\frac{N_{\rm df}}{2}, \frac{x}{2})$ is the lower incomplete gamma function, and $\Gamma(\frac{N_{\rm df}}{2})$ is the gamma function. This analysis results in a Nele family age of $3.6 \pm 1.6$ Myr. Note that this value is in good agreement with the value obtained in Section 4 (see Fig. 7, panel a) from considerations of the Nele family dispersal in secular angles forward in time. Fig. 9 shows the time dependence of $\Delta\chi^2$ and determination of the 95 per cent confidence level interval.

Our simulation described above, in which we included only the gravitational perturbations from planets, proved the tendency of Nele-family orbits to converge within the past million years in both secular angles. Still, the best attained level of $\simeq 36^\circ$ at which nodes and pericentres statistically approached the reference orbit of (1547) Nele or (4652) Iannini is quite large. Recall that the initial conditions at the family formation should produce a scatter of only a fraction of a degree. Obviously, the effects of orbital chaos and additional gravitational perturbers, such as massive asteroids, imply our simulation was not perfect and, presumably, when these are included the convergence would be improved. Additionally, previous studies demonstrated that especially for small members in the families, those with $D \leq 2$–3 km, one needs also to account for the thermal accelerations known as the Yarkovsky effect (e.g. Bottke et al. 2002; Vokrouhlický et al. 2015). Nesvorný & Bottke (2004) have shown that the Yarkovsky effect does not primarily perturb the secular angles of the orbits in a direct way. Instead, the influence is indirect by secularly changing the orbital semimajor axis $a$. This is because the precession rate of these angular variables due to the planetary perturbations sensitively depends on the orbital semimajor axis, and therefore the Yarkovsky change in $a$ propagates into the $\Omega$ and $\varpi$ values. In what follows, we thus aim at implementing this improvement, and we try to refine the orbital convergence of Nele members by accounting for the Yarkovsky effect in their orbital evolution.

The Yarkovsky effect depends on a number of physical parameters, including the spin state and surface thermal inertia, which are not known for virtually all Nele members. The only information we were able to find in the literature is the pole orientation for (1547) Nele that implies its obliquity to be $50^\circ \pm 15^\circ$ (Ďurech et al. 2016). We shall use this constraint, but for all other asteroids in the family we must account for a range of possible Yarkovsky effect values. This way for each body we consider a certain number of Yarkovsky clones (for more details see e.g. Carruba et al. 2016, 2017). In particular, we estimate the maximum Yarkovsky drift-rate $\mathrm{d}a/\mathrm{d}t$ for (1547) Nele to be $1.5 \times 10^{-11}$ au yr$^{-1}$ (e.g. Bottke et al. 2002; Vokrouhlický et al. 2015). Because the diurnal variant of the Yarkovsky effect typically dominates the seasonal, the $\simeq 50^\circ$ obliquity of this body implies a drift-rate of $1.5 \times 10^{-11} \cos 50^\circ \simeq 9.6 \times 10^{-12}$ au yr$^{-1}$. Note that, when applied for the backward integration the sign of $\mathrm{d}a/\mathrm{d}t$ has to be reversed in our simulation. Each other body in the Nele family was represented by 71 Yarkovsky clones with $\mathrm{d}a/\mathrm{d}t$ values uniformly sampling a range between minimum and maximum estimated drift-rates scaled from that of (1547) Nele, i.e. following the $\mathrm{d}a/\mathrm{d}t \propto 1/D$ dependence on size $D$ (e.g. Bottke et al. 2002; Vokrouhlický et al. 2015).

The whole sample of 24212 Yarkovsky clones (one for 1547 Nele) were numerically integrated backward in time over a 21 Myr interval using `SWIFT_RMVS3_DA`. This code derives from the `SWIFT_RMVS3` package in the swift family and has additionally an implementation of the Yarkovsky effect as described in Nesvorný & Bottke (2004). We again used a 10 d timestep and output data every $10^3$ yr. Post-processing Fourier filtering techniques, similar to those mentioned above, allowed us to remove high-frequency noise in the angular differences $\Delta\varpi$ and $\Delta\Omega$ of all clones with respect to the reference orbit of (1547) Nele.

Out of the 71 clones of each particle, we then selected the one that showed the best convergence to the reference orbit of (1547) Nele at each timestep. Using the target function in equation (3), we first obtained an estimate of the minimum $(\chi_0{}^2)_{\rm min} = 17.27$ rad$^2$ at 5.7 Myr. We then repeated the method outlined above, namely assigned a formal uncertainty $\sigma$ of the data points. For the case of the simulation that includes the Yarkovsky effect, the number of degrees of freedom is now $N_{\rm df} = 2(N_{\rm ast} - 1) - (N_{\rm ast} - 1) - 1 = N_{\rm ast} - 2$, since there were $2\,(N_{\rm ast} - 1)$ number of pairs contributing by angular differences, one estimated parameter (the family age) and we selected the best Yarkovsky clone for $N_{\rm ast} - 1$ family members (formally fitting the relevant $\mathrm{d}a/\mathrm{d}t$ values). Using equation (4)

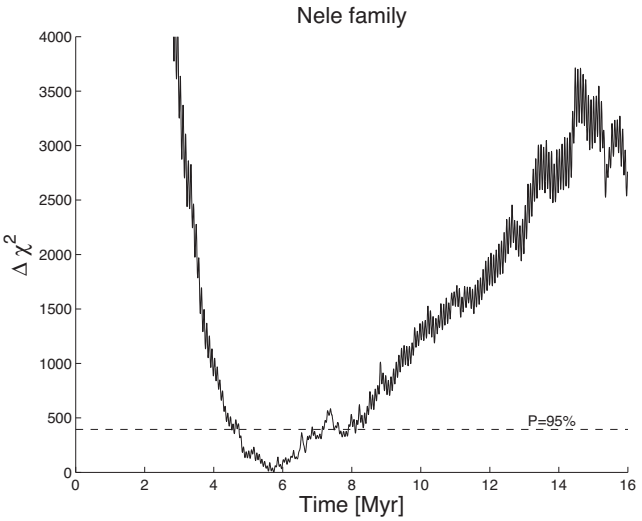


**Figure 10.** The time behaviour of $\Delta\chi^2 = \chi^2 - \chi^2_{\rm min}$ variable defined in equation (5) for a dynamical model where the thermal accelerations were taken into account. At each timestep, $10^3$ yr, we selected the optimum Yarkovsky drift-rate $da/dt$ for each Nele members (except for 1547 Nele, which has a constant value) in order to minimize $\chi^2$ value. The formal minimum with $\chi^2_{\rm min} \simeq 1$ occurs for 5.7 Myr epoch. The 95 per cent probability confidence level is shown by the dashed horizontal line.

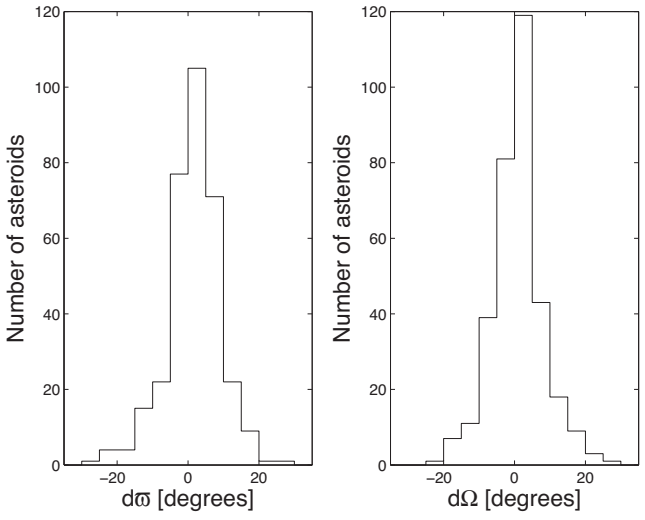


**Figure 11.** Distributions of $\Delta\varpi$ and $\Delta\Omega$ of the best Yarkovsky clones at the Nele family formal age in our solution with the thermal accelerations included. Standard deviation of both variables is $\simeq 7\overset{\circ}{.}3$, indicating a significant improvement compared to the solution without the thermal effects.

with this new value of $N_{\rm df} = 340$, we obtained $\sigma^2 \simeq 0.050$ rad$^2$, or $\sigma \simeq 12\overset{\circ}{.}9$. This is now a much better convergence solution than before, obviously the result of the Yarkovsky effect contribution to the secular angles evolution (especially for smaller members in the family). Note, however, that the $\sigma$ value is still at least an order of magnitude larger than expected from the initial dispersion of secular angles in the Nele family. The remaining mismatch is likely due to the gravitational effects of massive bodies in the main belt and overall chaotic dynamics in this zone of orbital phase space. It is also possible that some of the Yarkovsky drift-rates $da/dt$, assigned to the clones in our second simulation, were overestimated to compensate these remaining dynamical effects that were not included in our model.

Applying now the best-fitting $\sigma$ value to equation (5), a non-dimensional $\chi^2$ target function, we can again formally follow the least-square method to determine the fitted parameters. As mentioned above, at each timestep at which results were output from our simulation (i.e. $10^3$ yr), we selected the best possible $da/dt$ value of each of the Nele asteroids to obtain minimum $\chi^2_0$ or $\chi^2$ value. This way we separate the solution of the family age from the solution of the Yarkovsky drift-rates, withdrawing the possibility of proper correlations of these many parameters. As above, we formally construct $\Delta\chi^2 = \chi^2 - \chi^2_{\rm min}$ using equation (5) as a function of time (see Fig. 10). For $N_{\rm df} = 340$, the 95 per cent confidence level corresponds to $\Delta\chi^2 \simeq 394.6$ (equation 6).

As seen in Fig. 10, at this confidence level we would conclude that the Nele family is $5.7^{+1.5}_{-1.3}$ Myr, which barely overlaps with the time interval found in the conservative simulation (i.e. $3.6 \pm 1.6$ Myr). Recall also that an age older than 4.5 Myr seems unlikely in view of the current clustering of $\varpi$ angles for the largest members ($H < 16$) of the Nele family, as discussed in Section 4. Therefore, the difference in the formal age values obtained with the conservative simulation and, especially, the one including the Yarkovsky effect requires some consideration. One possibility of the discrepancy, advocated below, is due to an asymmetric distribution of the Yarkovsky drift rates of the Nele family.

Before we go to this speculative issue, we first show the distribution of $\Delta\varpi_i$ and $\Delta\Omega_i$ values for the formally best-fitting solution at 5.7 Myr epoch in the past (the differences are with respect to the orbit of (1547) Nele; Fig. 11). The standard deviation of both distributions is small, namely $7\overset{\circ}{.}3$ and $7\overset{\circ}{.}2$, which is at the above estimated level $\sigma \simeq 12\overset{\circ}{.}9$. This confirms the ability of the dynamical model to result in a much better convergence level than the purely gravitational model above. Interestingly, the initial asymmetry of the longitude of perihelion of (1547) Nele with respect to the largest asteroids in its family has been well absorbed in the solution (note the mean value of $\Delta\varpi_i$ on the left-hand panel of Fig. 11 is fairly close to zero).

Next, we analysed the semimajor axis drift-rates $da/dt$ for the Yarkovsky clones selected at the best-fitting age solution at 5.7 Myr ago. Fig. 12 shows their values as a function of the body's size $D$. By definition, the $da/dt$ values for the clones are bound in the minimum/maximum interval estimated from the linear Yarkovsky theory (e.g. Bottke et al. 2002; Vokrouhlický et al. 2015). The fact that these values do not pile-up towards the extreme values is a good sanity check. Instead, they are roughly uniformly distributed within allowed limits with: (i) a preference towards negative $da/dt$ values ($\simeq$61 per cent of the sample), and (ii) a slight deficit values near $da/dt \simeq 0$ for small Nele members ($D \leq 1.5$ km, say). The first, may be explained by a small contribution of the seasonal variant of the Yarkovsky effect as noted in the case of the Veritas family by Carruba et al. (2017). However, it could also result from an initial anisotropy of the rotation poles of Nele members having, for instance, preferentially obliquities larger than 90°. The second feature in Fig. 12, notably lack of $da/dt \simeq 0$ values for small Nele members, could be indicative of the YORP effect tilting obliquities of the asteroids towards extreme values as first detected in the case of the Karin family by Carruba et al. (2016). Note, however, that these results should be taken with a reserve. This is because a proper analysis of the uncertainties of the determined $da/dt$ values would likely indicate they basically span the whole available interval of values.

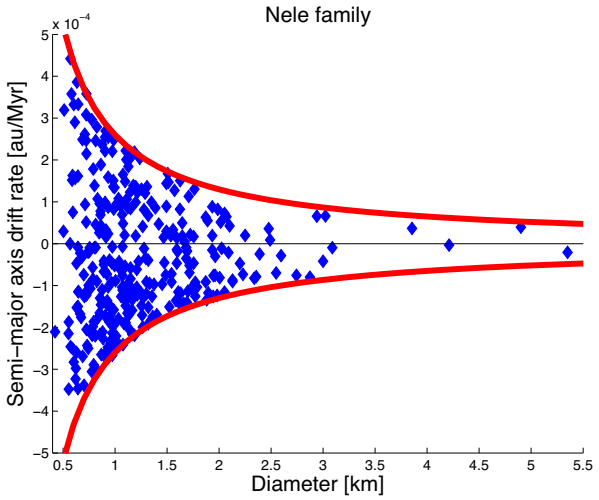


**Figure 12.** Semimajor axis drift-rates d$a$/d$t$ for 321 Nele family members with $D \leq 5.5$ km. These values correspond to the best-fitting convergence of the family at 5.7 Myr ago (see Fig. 10). Red lines show the estimated limiting values from the linearized theory of the Yarkovsky effect.

As a further check, we also determined the distribution of d$a$/d$t$ values for younger ages of the Nele family. For example, when it is assumed that the Nele family is 3.6 Myr old (the formal best solution in a model where only the gravitational perturbations were taken into account), the distribution of d$a$/d$t$ becomes skewed towards negative values with many asteroids having values near the maximum drift rate permitted by the Yarkovsky theory. Such a non-random distribution would be unusual. This is probably related to the fact that Nele itself is offset in both angles from the rest of the family at the present time (see Fig. 5). This observation may, though, explain the difference in the formal Nele ages in our two models discussed in this section. Assume, for instance, that the true initial distribution of obliquities in the Nele family was skewed towards values larger than 90°, with some d$a$/d$t$ values even exceeding our conservative limits. Our model with the thermal accelerations included would not find these solutions near the nominal age in the gravitational-only model. Rather, the formal age would be pushed to older values where convergence would be achieved at the expense of a more symmetric, but false, set of the Yarkovsky clones. Without additional information, however, we cannot decide which of the cases is correct and we do not have an a priori reason to reject formal solutions with the Nele age slightly exceeding 5–6 Myr.

## 6 CONCLUSIONS

Our results could be summarized as follows.

(i) We revisited the Nele family membership by using the most up-to-date catalogue of proper orbital elements, updating thus earlier findings in Milani et al. (2014) and Nesvorný et al. (2015). The Nele family is a very compact cluster of asteroids in a rather isolated zone of the central main belt. No other important asteroid clusters were found in Nele vicinity, making thus the analysis of this family easier. None of the linear or principal non-linear secular resonances play an important role in the dynamical evolution of the Nele group. Moderate level of chaoticity of orbits in the Nele family, revealed by LCE, is likely related to unusual three-body resonances not involving planet Jupiter, four-body resonances, or two-body resonances with Venus.

(ii) We also reviewed the physical properties of asteroids in the Nele region, finding the available data are still rather scarce. Only seven objects have taxonomic information from SDSS, and only 14 have *WISE*, *NEOWISE*, *AKARI*, or *IRAS* albedo data. Based on this limited information, we find that the Nele family is an S-type family, confirming previous analysis. The probable largest fragment of its namesake family, namely asteroid (1547) Nele, however shows some irregularity: (i) its spectrum has been preliminarily classified as TD in Tholen's taxonomic scheme, and (ii) its geometric albedo was found 0.20, significantly lower then for other members in the cluster. It is possible, though, that both these data are uncertain, and more observations of this asteroid will be needed to clarify this issue.

(iii) The Nele family is rare among its class by indicating statistical clustering of the longitude of perihelion and node in orbits of the largest members (e.g. Nesvorný et al. 2003). This property indicates its youth. Forward integration of a synthetic Nele family suggests the observed clustering of the perihelia is consistent with an age smaller than 4.5 Myr. The age may be also estimated by the V-shape method discussed in Spoto et al. (2015), notably by interpreting slope of the delimiting lines of the family in the ($a$, $1/D$) plane of parameters [the equivalent method in the ($a$, $H$) plane was introduced by Vokrouhlický et al. 2006a. This would result in an age of $\simeq$15 Myr, neglecting the effect of initial fragment dispersal. On a flip side of the same coin, one could neglect the orbital evolution of the family fragments by the Yarkovsky effect and use the ($a$, $1/D$) data to estimate the characteristic speed at which the fragments in the Nele family were initially ejected from the parent body. This would lead to $\simeq$17 m s$^{-1}$. The reality is a combination of the two effects. Observing that the estimated escape velocity from (1547) Nele is $\simeq$10 m s$^{-1}$, the likely partition is 2 : 1 in favour of the initial velocity effect. This would consistently come back to the rough age estimate of $\simeq$5 Myr.

(iv) Inspired by previous success in the case of Karin and Veritas families (and also a set of very small and young families reported, e.g. in Nesvorný & Vokrouhlický 2006), we attempted to improve the age estimate for the Nele family by numerical propagation of its orbits backward in time. The goal of this approach is to achieve as close convergence of the orbits as possible, in our case monitored by behaviour of the secular angles only. We conducted two such simulations: (i) first, including only the gravitational perturbations of the planets, and (ii) secondly, including additionally the dynamical effects of the thermal accelerations. Each time, we numerically integrated the orbits of 342 members in the Nele family backward in time for 20 Myr. The first set of runs, with gravitational perturbations included, lead to a poorer convergence. At best, the perihelia and nodes statistically approached the orbit of (1547) Nele to about 36°. Assuming this is a reasonable limit of the simple model, we concluded that the Nele family is 3.6 $\pm$ 1.6 Myr old. As expected, the second model where thermal accelerations were modelled for each of the 342 asteroids in the family lead to significant improvement of the convergence. At best, our solutions achieved $\simeq$7.°5 convergence level of perihelii and nodes. The nominal age found with the integration including Yarkovsky drift rates is $5.7^{+1.5}_{-1.3}$ Myr, barely compatible with the gravitational-only solution above. We suspect that the age difference in our two models may be due to a preferentially retrograde spin state of many fragments in this family.

Our analysis confirmed the very young age of the Nele family. This implies that it remains the best source candidate of the J/K dust band at $\simeq$12° proper inclination (e.g. Nesvorný et al. 2003). An improvement of the Nele age estimate may require a priori constraints

on some, or all, of the free parameters in the model. For instance, if we were to know obliquity values for some Nele members, the solution will likely be quite more deterministic. At first sight this may look like science fiction, however, we note the enormous improvements in pole solutions for many main belt asteroids (e.g. Ďurech et al. 2015). Assuming that high-quality sparse photometry from ground- and space-based upcoming surveys will become available, we may expect pole solutions for thousands (if not more) of main belt objects.

## ACKNOWLEDGEMENTS

We are grateful to Andrea Milani and to the reviewer of this paper, Bojan Novaković, for comments and suggestions that helped to improve the quality of this paper. We would like to thank the São Paulo State Science Foundation (FAPESP) that supported this work via the grants 16/04476-8 and 2013/15357-1, and the Brazilian National Research Council (CNPq, grant 305453/2011-4). DV's work was funded by the Czech Science Foundation through the grant GA18-06083S. DN's work was supported by the NASA SSW programme. VC was a visiting scientist at the Southwest Research Institute while some of the research for this work was developed. We acknowledge the use of data from the Asteroid Dynamics Site (AstDyS) (http://Hamilton.dm.unipi.it/astdys; Knežević and Milani 2003). This publication makes also use of data products from the *Wide-field Infrared Survey Explorer* (*WISE*) and Near-Earth Objects (NEOWISE), which are a joint project of the University of California, Los Angeles, and the Jet Propulsion Laboratory/California Institute of Technology, funded by the National Aeronautics and Space Administration.

## REFERENCES

Bendjoya P., Zappalà V., 2002, in Bottke W. F., Cellino A., Jr, Paolicchi P., Binzel R. P., eds, Asteroids III. Univ. Arizona Press, Tucson, AZ, p. 613
Bolin B. T., Walsh K. J., Morbidelli A., Delbò M., 2018, MNRAS, 473, 3949
Bottke W. F., Vokrouhlický D., Rubincam D. P., Brož M., 2002, in Bottke W. F., Jr, Cellino A., Paolicchi P., Binzel R. P., eds, Asteroids III. Univ. Arizona Press, Tucson, AZ, p. 395
Brož M., 1999, Thesis, Charles University
Brož M., Morbidelli A., Bottke W. F., Rozehnal J., Vokrouhlický D., Nesvorný D., 2013, A&A, 551, A117
Carruba V., 2010, MNRAS, 408, 580
Carruba V., Nesvorný D., 2016, MNRAS, 457, 1332
Carruba V., Burns J. A., Bottke W. F., Nesvorný D., 2003, Icarus, 162, 308
Carruba V., Nesvorný D., Vokrouhlický D., 2016, AJ, 151, 164
Carruba V., Vokrouhlický D., Nesvorný D., 2017, MNRAS, 469, 4400
Carry B., 2012, Planet. Space Sci., 73, 98
Chesley S. R. et al., 2014, Icarus, 235, 5
DeMeo F. E., Carry B., 2013, Icarus, 226, 723
Ďurech J., Carry B., Delbò M., Kaasalainen M., Viikinkoski M., 2015, in Michel P., DeMeo F. E., Bottke W., eds, Asteroids IV. Univ. Arizona Press, Tucson, AZ, p. 183
Ďurech J., Hanuš J., Oszkiewicz D., Vančo R., 2016, A&A, 587, A48
Gallardo T., 2014, Icarus, 231, 273
Ishihara D. et al., 2010, A&A, 514, A1
Ivezić Ž. et al., 2001, AJ, 122, 2749
Knežević Z., Milani A., 2003, A&A, 403, 1165
Levison H. F., Duncan M. J., 1994, Icarus, 108, 18
Mainzer A. et al., 2016, VizieR Online Catalog, 178
Masiero J. R., Mainzer A. K., Grav T., Bauer J. M., Jedicke R., 2012, ApJ, 759, 14
Milani A., Cellino A., Knežević Z., Novaković B., Spoto F., Paolicchi P., 2014, Icarus, 239, 46
Nesvorný D., Bottke W. F., 2004, Icarus, 170, 324
Nesvorný D., Morbidelli A., 1998, AJ, 1163, 3029
Nesvorný D., Vokrouhlický D., 2006, AJ, 132, 1950
Nesvorný D., Bottke W. F., Dones L., Levison H. F., 2002, Nature, 417, 720
Nesvorný D., Bottke W. F., Levison H. F., Dones L., 2003, AJ, 591, 486
Nesvorný D., Brož M., Carruba V., 2015, in Michel P., DeMeo F. E., Bottke W., eds, Asteroids IV. Univ. Arizona Press, Tucson, AZ, p. 297
Novaković B., 2010, MNRAS, 407, 1477
Press V. H., Teukolsky S. A., Vetterlink W. T., Flannery B. P., 2001, Numerical Recipes in Fortran 77. Cambridge Univ. Press, Cambridge
Ryan E. L., Woodward C. E., 2010, AJ, 140, 933
Sheskin D. J., 2003, Handbook of Parametric and Nonparametric Statistical Procedures, Fourth Edition. Elsevier, Amsterdam
Spoto F., Milani A., Knežević Z., 2015, Icarus, 257, 275
Vokrouhlický D., Brož M., Bottke W. F., Nesvorný D., Morbidelli A., 2006a, Icarus, 182, 92
Vokrouhlický D., Brož M., Bottke W. F., Nesvorný D., Morbidelli A., 2006b, Icarus, 183, 349
Vokrouhlický D., Bottke W. F., Chesley S. R., Scheeres D. J., Statler T. S., 2015, in Michel P., DeMeo F. E., Bottke W., eds, Asteroids IV. Univ. Arizona Press, Tucson, AZ, p. 509

This paper has been typeset from a TEX/LATEX file prepared by the author.